Computational Sciences and Engineering 2(1) (2022) 69-79

University of Guilan

Computational Sciences and Engineering

journal homepage: https://cse.guilan.ac.ir/

Convolutional Neural Networks with Different Dimensions for POLSAR Image Classification

Maryam Imani [a,*]

[a] Faculty of Electrical and Computer Engineering, Tarbiat Modares University, Tehran, Iran

ARTICLE INFO

Article history:
Received 5 March 2022
Received in revised form 19 March 2022
Accepted 15 April 2022
Available online 20 April 2022

Keywords:
PolSAR
Classification
feature extraction
CNN

ABSTRACT

Polarimetric Synthetic aperture radar (PolSAR) images contain polarimetric and spatial information of materials present in the scene. Three simple architectures of convolutional neural networks (CNNs) with different dimensions are proposed for PolSAR image classification in this work. A one dimensional CNN (1D CNN) is suggested for polarimetric feature extraction. A 2D CNN is presented for spatial feature extraction and a 3D CNN is introduced for polarimetric-spatial feature extraction. The performance of CNNs are compared with morphological profile of PolSAR cube when fed to the support vector machine (SVM) and random forest (RF) classifiers. The experiments are done in two cases of using 1% and 5% training samples. The superiority of 3D CNN compared to other methods is shown using different quantitative classification measures.

1. Introduction

Synthetic aperture radar (SAR) sensors provide high resolution images from the earth under day and night and any weather conditions. Polarimetric SAR (PolSAR) by acquiring SAR images in different polarization states allows more accurate discrimination between various materials on the earth [1].

The available classifiers are divided into two main groups: 1- manually classifiers designed based on statistics or a specific optimization problem, and 2- intelligent classifiers inspired from human brain. Maximum likelihood [2], support vector machine (SVM) [3] and random forest (RF) [4] are examples of the first group and various neural networks belong to the second one [5]. In the first type of classifiers, the required feature extraction has to be done separately. The separately extracted features may not bet so suitable and matched with the used classifier. The use of features together with inappropriate classifier may decrease the classification accuracy. In contrast, in the second type

* Corresponding author.
E-mail addresses: maryam.imani@modares.ac.ir (M. Imani)

http://dx.doi.org

of classifiers, both feature extraction and classification is done in a unified framework which is an important benefit.

Deep learning has opened a new vision in machine learning that has improved the efficiency of conventional neural networks. Deep neural networks recently attract attention in various remote sensing applications [6]. Deep networks automatically extract robust and invariant features in high levels. PolSAR image classification using deep networks has been also done in several works. In [7], the PolSAR image is converted to a six-channel image with real values. Then, the real cube is fed to a two-dimensional convolutional neural network (2D CNN) for extraction of hierarchical spatial features. In [8], three known models (VGG-16, ResNet-50 and DenseNet-121) pretrained with the large ImageNet dataset are used for PolSAR image classification by proposing an ensemble transfer learning. In [9], a polarimetric scattering coding is proposed to provide a complete polarimetric feature set. Then, the extracted features are fed to a designed 2D-CNN for classification.

One drawback of 2D CNN is its weak capacity in feature extraction in polarization or scattering dimension. To deal with this issue, 3D CNN has been suggested [10]. But, it has used the real values and lost the phase information. The work in [11] has introduced complex valued 3D CNN to benefit both real and imaginary parts of PolSAR image.

In this paper, three CNNs with simple architectures, 1D CNN, 2D CNN and 3D CNN, are proposed where polarimetric features, spatial features and polarimetric-spatial features are extracted by them, respectively. The CNNs with different dimensions are compared with SVM and RF classifiers in two different cases. In the first case, the PolSAR cube is fed to the SVM and RF. In this case, just polarimetric features are used. To include the spatial information, the morphological profile (MP), which obtain great successful in spatial feature extraction from remote sensing images [12], is employed in the second case. The stacked PolSAR cube with the computed MP are used as the input of SVM and RF classifiers in the second case. The performance of CNNs are compared with their competitors using small training sets and the results obtained by a real PolSAR image are discussed.

2. Polarimetric and spatial feature extraction using CNN

One of the main difficulties in the used conventional CNNs is overfitting problem. It is due to the high number of trainable parameters of the network and the low number of training samples. To overcome to this difficulty, three CNNS with the following characteristics are proposed:

1- Just two convolutional layers are used in the networks to reduce the number of trainable parameters.
2- The conventional CNNs use the pooling layer to reduce the data size. But, the use of pooling layer discard some useful extracted features. In the proposed networks, pooling layers are deleted; and instead of them, the convolutional filters with a stride of 2 are used.
In this section, at first, the form of PolSAR image is presented. Then, different dimensions of CNNs are introduced for extracting polarimetric features, spatial features or both of them as follows:

1D CNN: polarimetric feature extraction
2D CNN: spatial feature extraction
3D CNN: polarimetric-spatial feature extraction

2.1. PolSAR image

A PolSAR system transmits polarized radar pulses horizontally (H) or vertically (V) and receives their coherences. Due to scattering of incident electromagnetic on objects and materials on the ground, the polarization state of the incident wave is altered. This alteration is a function of geometrical and physical characteristics of materials which can be served to characterize them. The scattering matrix for each cell of SAR image has the following form:

$$\boldsymbol{S} = \begin{bmatrix} S_{HH} & S_{HV} \\ S_{VH} & S_{VV} \end{bmatrix} \tag{1}$$

where S_{ij} is known as the scattering coefficient, i is the polarization of transmitting and j denotes that of receiving value. Reciprocity of objects or targets is a common assumption in polarimetry. So, the scattering matrix can be constrained to be symmetric, i.e., $S_{VH} = S_{HV}$ in the symmetric monostatic scattering. The scattering vector $\boldsymbol{k}$ can simplify the scattering matrix by:

$$\boldsymbol{k} = \frac{1}{\sqrt{2}}[S_{HH} + S_{VV} \quad S_{HH} - S_{VV} \quad 2S_{HV}]^T \tag{2}$$

where T denotes the transpose operation. Then, the coherency matrix for multilook case is expressed as follows:

$$\boldsymbol{T} = \frac{1}{L}\sum_{i=1}^{L} \boldsymbol{k}_i \, \boldsymbol{k}_i^H \tag{3}$$

$$\boldsymbol{T} = \begin{bmatrix} T_{11} & T_{12} & T_{13} \\ T_{21} & T_{22} & T_{23} \\ T_{31} & T_{32} & T_{33} \end{bmatrix} \tag{4}$$

where L is the number of looks and H represents the conjugate transpose. The coherency matrix is Hermitive with real values in diagonal elements and complex ones in off-diagonal ones. The following vector is considered as the feature vector of each pixel of PolSAR image [13]:

$$\boldsymbol{f} = [T_{11}, T_{22}, T_{33}, Re(T_{12}), Im(T_{12}), Re(T_{13}), Im(T_{13}), Re(T_{23}), Im(T_{23})] \tag{5}$$

where $Re(\cdot)$ and $Im(\cdot)$ denote the real and imaginary parts of $(\cdot)$, respectively. These 9 features obtained by coherency matrix contain polarimetric information of PolSAR image. A PolSAR image with N rows and M columns can be represented by a $N \times M \times 9$ cube where there are spatial information in two dimensions and polarization information in the third dimension.

2.2. 1D CNN

CNNs have two main useful characteristics: shared weights and local connections which lead to better generalization and overcoming to overfitting problem. Each convolutional filter does convolutional operation only for a part of neighboring neurons (receptive filed). The local connectivity among neurons of near layers is used to exploit the local correlation. To apply 1D CNN

to PolSAR image, the polarization vector of each pixel that is a 9×1 vector is given as an input of network. By applying convolutional operator to local parts of polarimetric feature vector, robust and invariant polarimetric features are produced. The relation and correlation among coherency elements which involve various polarization states of pixel is also extracted. Figure 1, shows the blockdiagram of the PolSAR image classification using 1D CNN. In the1D CNN, pixels are imported to the network one by one. The number and size of used kernels are shown in the figure.

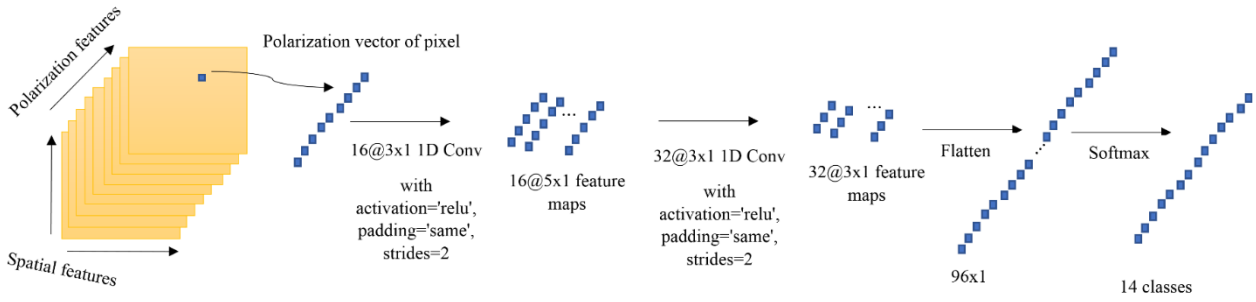

Figure. 1. PolSAR image classification using 1D CNN.

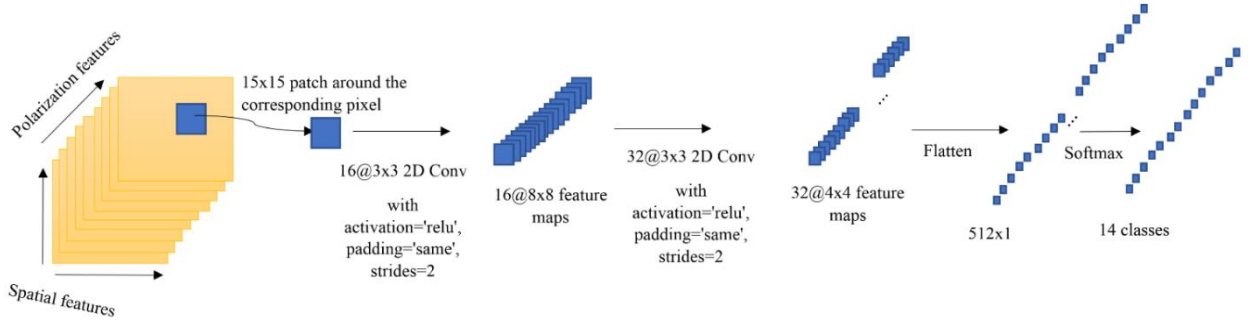

Figure 2. PolSAR image classification using 2D CNN.

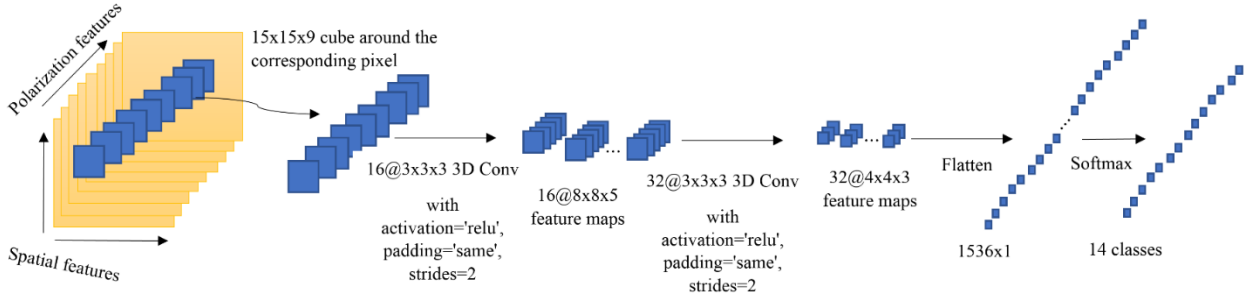

Figure 3. PolSAR image classification using 3D CNN.

2.3. 2D CNN

In the1D CNN, each pixel of PolSAR image with a 9×1 polarimetric vector is fed to the network to extract more abstract polarimetric features in high level. But, PolSAR data in each captured polarization or in each channel obtained from the coherence matrix, is a high resolution image. If consider the PolSAR cube as a multi-channels image, each channel contains valuable spatial information such as shape, texture and geometrical characteristics. 1D CNN is not able to extract this rich spatial information. To deal with this problem, the 2D CNN has been suggested.

One of the main capabilities of convolutional networks compared to fully connected ones is ability of them in handling of image data in two dimensions. While in traditional fully connected neural networks, only accepted form of input is vector, 2D CNN can accept image data in the same form of two-dimensions instead of stacking pixels together.

The blockdiagram of the suggested 2D CNN is illustrated in Figure 2. Around the given pixel, a 15×15 patch is considered and imported to the input of 2D CNN. The 2D convolutional operators extract high level spatial features in subsequent layers.

2.4. 3D CNN

While 1D CNN extracts the polarimetric features, 2D CNN extracts the spatial features. But, simultaneously extraction of polarimetric and spatial features can be a more effective way for increasing separability among different classes. 3D CNN is used as a solution. Figure 3 shows the architecture of the suggested 3D CNN. The considered 15×15×9 cube around each pixel is given as input of the 3D CNN. The 3D convolutional operators can extract more abstract polarimetric-spatial features in subsequent layers.

3. Experiments

A real benchmark PolSAR dataset, which acquired by AIRSAR in L-band in 1991 [13], is used for doing experiments. This agriculture PolSAR image acquired from Flevoland in Netherlands contains 14 classes and 1020×1024 pixels. The performance of 1D CNN, 2D CNN and 3D CNN is compared with four state-of-the-art classifiers:

- SVM (POL): the support vector machine classifier (SVM). Its input is the polarization SAR cube (POL) where feature representation of it for each pixel is represented in (5).
- SVM (POL+MP): the SVM classifier where its input is the stacked polarization cube (POL) with the morphological profile (MP). “+” means stacking here.
- RF (POL): the random forest (RF) classifier with POL as input.
- RF (POL+MP): the RF classifier with POL+MP as input.

To provide the MP, at first, the principal component analysis transform [14] is applied to the PolSAR cube. The first three principal components (PCs) that contain the most of energy of data are selected. Then, a MP is made from each PC. To this end, 26 opening filters and 26 closing filters with structure element of circle are applied to each PC. Thus, a MP with 26×2+1=53 dimensions is created from each PC. The obtained MPs are stacked together to form the final MP. The third degree polynomial kernel is used for implementation of SVM. 70 bagged classification trees are used for

implementation of RF. RF and SVM are implemented in MATLAB R2018b and CNNs are implemented using Keras in Tensorflow backend.

The performance of different classifiers are assessed in two different cases: 1- when 1% of labeled samples are used as training samples and 2- when 5% of labeled samples are used as training samples. The number of training samples in two cases are represented in Table 1. To obtain the full classification maps, all samples of PolSAR image are used in the testing process. But, just the samples with label in ground truth map (GTM) are involved in calculation of classification accuracy. Average accuracy, average reliability, overall accuracy and kappa coefficient [15] are used for evaluation. In addition, to assess the performance of classifiers from the statistical point of view, the McNemars test [16] is done and the Z values are reported in the paper. The difference between classification accuracy of two methods is significant if $|Z_{12}| > 1.96$. $Z_{12} > 0$ means method 1 is preferred than method 2 and vice versa.

Table 1. The number of training samples in Flevoland dataset.

No	Name of class	# samples	# Training samples (1%)	# Training samples (5%)
1	Potato	21613	217	1081
2	Fruit	4352	44	218
3	Oats	1394	14	70
4	Beet	10817	109	541
5	Barley	24543	246	1228
6	Onions	2130	22	107
7	Wheat	26277	263	1314
8	Beans	1082	11	55
9	Peas	2160	22	108
10	Maize	1290	13	65
11	Flax	4301	44	216
12	Rapeseed	28235	283	1412
13	Grass	4204	43	211
14	Lucerne	2952	30	148
Total		135350	1361	6774

The loss versus the number of epochs for both training and validation sets obtained by 1D CNN, 2D CNN and 3D CNN for 1% training samples are shown in Figures. 4-6, respectively. As seen, the plots of 3D CNN converge faster than 1D CNN and 2D CNN, i.e., becomes stable in lower number of epochs.

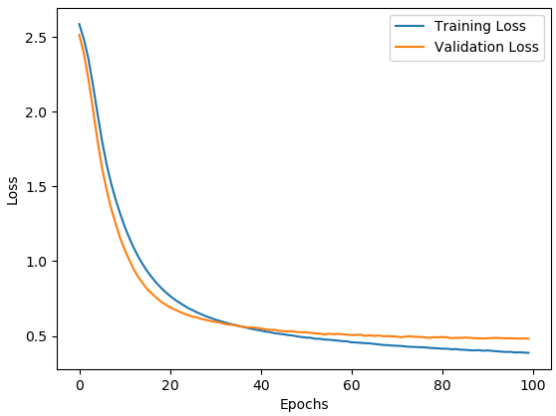

Figure 4. Loss and accuracy obtained by 1D CNN.

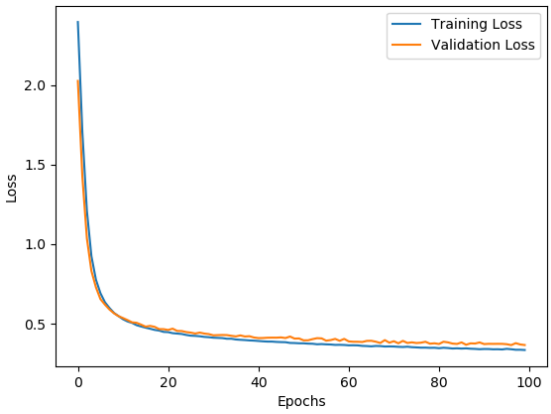

Figure 5. Loss and accuracy obtained by 2D CNN.

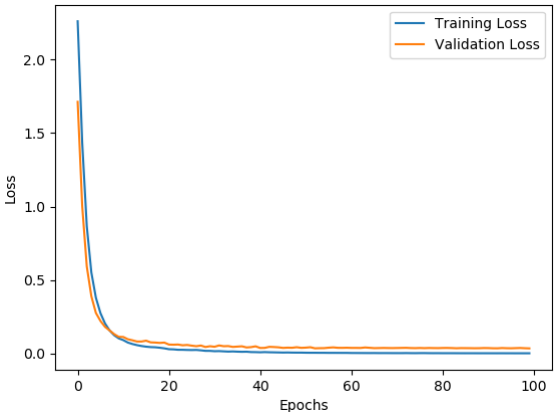

Figure 6. Loss and accuracy obtained by 3D CNN.

The classification results and its associated McNemars results for 1% training samples are reported in Table 2 and 3, respectively. The RGB image beside the obtained classification maps are shown in Figure 7. The results achieved by 5% training samples are represented in Tables 4-5 and Figure 8. The following results can be concluded from the obtained results:

1- Superiority of 2D CNN and 3D CNN with respect to 1D CNN is obvious. It is expected because 1D CNN ignores the valuable shape, texture and geometrical information contained in two spatial dimensions.
2- 3D CNN provides the best classification results. It extracts high level polarimetric-spatial features that can increase the class discrimination.
3- Difference between 2D CNN and 3D CNN using 1% training samples is more than that using 5% training samples. According to the McNemars test results, difference in classification accuracy between 2D CNN and 3D CNN is not significant from the statistical point of view using 5% training samples.
4- SVM and RF generally provide better classification results with respect to 1D CNN.
5- Using 1% training samples, RF (POL) is preferred than SVM (POL) while SVM (POL+MP) works better than RF (POL+MP). In the case of POL+MP, the dimensionality of data is high and SVM has higher ability for dealing with the curse of dimensionality.
6- Using 5% training samples, RF is preferred than SVM in both cases of POL and POL+MP.

Table 2. Classification results achieved by 1% training samples.

class			SVM (POL)		SVM (POL+MP)		RF (POL)		RF (POL+MP)		1D CNN		2D CNN		3D CNN	
No	Name of class	#samples	Acc.	Rel.	Acc.	Rel.	Acc.	Rel.	Acc.	Rel.	Acc.	Rel.	Acc.	Rel.	Acc.	Rel.
1	Potato	21613	89.52	86.02	98.16	98.94	89.82	85.11	98.14	98.55	85.73	88.33	99.97	99.66	99.80	99.09
2	Fruit	4352	79.20	87.60	98.05	99.42	71.81	91.88	98.25	100	78.47	79.23	99.45	99.98	99.33	99.54
3	Oats	1394	41.03	37.02	98.35	96.48	27.26	66.09	97.70	98.84	11.26	66.53	98.78	99.14	97.70	99.56
4	Beet	10817	90.92	82.38	96.33	95.34	89.15	84.01	93.01	94.66	93.41	71.53	92.47	98.21	97.47	95.45
5	Barley	24543	89.83	89.29	98.04	97.80	93.51	87.18	97.64	96.37	93.65	85.92	99.55	99.70	99.73	99.61
6	Onions	2130	17.14	31.12	77.89	82.78	22.82	38.33	81.64	88.77	7.09	27.31	64.93	59.97	63.76	81.07
7	Wheat	26277	93.52	88.09	98.37	98.20	93.23	88.87	98.96	97.23	91.44	90.60	99.76	99.13	99.33	99.08
8	Beans	1082	73.01	53.13	85.58	97.68	54.99	57.88	83.36	99.34	37.34	64.13	93.16	91.39	93.16	94.74
9	Peas	2160	49.91	82.48	97.04	94.03	67.69	87.97	99.77	96.68	72.82	78.97	99.77	99.35	97.13	100
10	Maize	1290	39.15	68.80	95.89	98.72	49.38	68.27	96.90	97.58	2.25	11.15	86.28	82.94	93.18	89.43
11	Flax	4301	91.40	94.29	96.65	99.40	82.05	92.84	98.21	99.81	83.89	87.17	99.33	99.79	98.35	100
12	Rapeseed	28235	91.02	90.18	98.21	96.86	91.45	88.83	97.72	95.34	91.72	88.66	99.89	99.60	99.93	99.07
13	Grass	4204	58.75	69.40	84.35	87.00	62.84	72.98	80.66	91.38	53.50	70.06	94.58	88.87	91.27	98.08
14	Lucerne	2952	54.61	83.96	88.25	86.37	54.03	87.88	78.35	86.60	66.06	80.05	95.39	99.61	99.25	94.33
Average Accuracy and Average Reliability			**68.50**	**74.55**	**93.65**	**94.93**	**67.86**	**78.44**	**92.88**	**95.80**	**62.04**	**70.69**	**94.52**	**94.10**	**94.96**	**96.36**
Overall Accuracy			**85.91**		**96.89**		**86.28**		**96.38**		**85.02**		**98.18**		**98.45**	
Kappa coefficient			**0.8334**		**0.9634**		**0.8373**		**0.9573**		**0.8227**		**0.9786**		**0.9818**	

Table 3. McNemars test results achieved by 1% training samples.

	SVM (POL)	SVM (POL+MP)	RF (POL)	RF (POL+MP)	1D CNN	2D CNN	3D CNN
SVM (POL)	0	-109.66	-4.56	-103.16	11.92	-121.39	-125.52
SVM (POL+MP)	109.66	0	107.98	9.93	115.55	-23.58	-30.33
RF (POL)	4.56	-107.98	0	-101.43	15.80	-119.12	-123.21
RF (POL+MP)	103.16	-9.93	101.43	0	109.24	-30.90	-37.37
1D CNN	-11.92	-115.55	-15.80	-109.24	0	-127.21	-131.05
2D CNN	121.39	23.58	119.12	30.90	127.21	0	-6.81
3D CNN	125.52	30.33	123.21	37.37	131.05	6.81	0

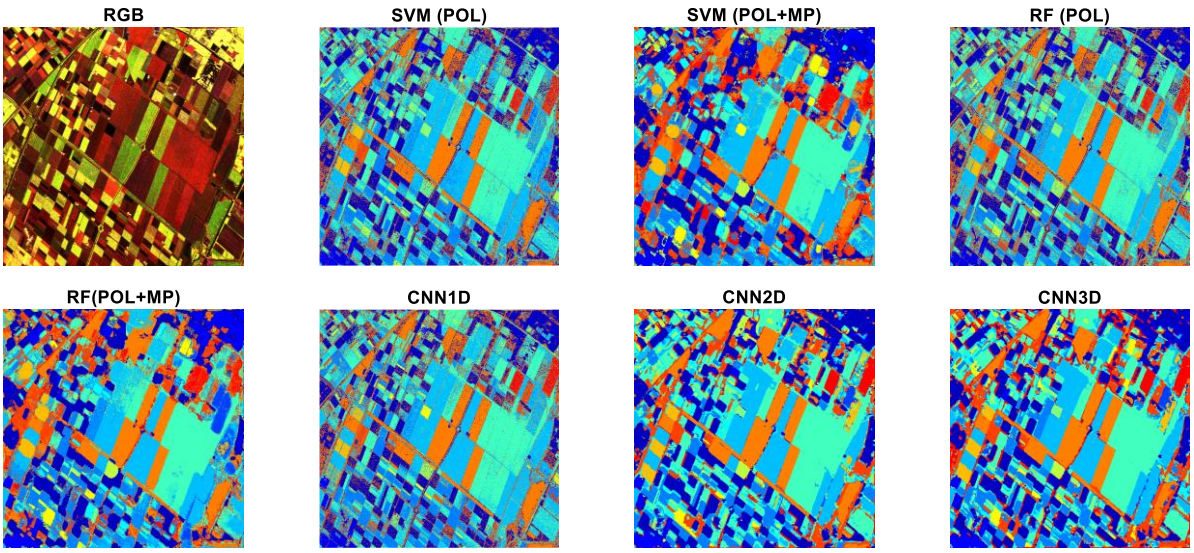

Figure 7. RGB image and classification maps achieved by 1% training samples.

Table 4. Classification results achieved by 5% training samples.

class			SVM (POL)		SVM (POL+MP)		RF (POL)		RF (POL+MP)		1D CNN		2D CNN		3D CNN	
No	Name of class	#samples	Acc.	Rel.	Acc.	Rel.	Acc.	Rel.	Acc.	Rel.	Acc.	Rel.	Acc.	Rel.	Acc.	Rel.
1	Potato	21613	90.94	88.60	99.23	99.39	90.52	88.73	99.39	99.80	90.08	90.03	99.99	99.83	99.81	99.99
2	Fruit	4352	78.10	89.61	99.59	99.98	78.29	90.76	99.75	100	84.79	84.30	100	99.98	99.95	99.07
3	Oats	1394	36.37	75.67	99.57	99.14	40.17	75.07	99.50	97.95	52.80	61.59	100	100	100	99.79
4	Beet	10817	92.90	83.60	98.19	97.79	92.35	86.41	98.97	98.97	91.35	85.63	98.96	99.05	99.31	99.29
5	Barley	24543	93.96	90.09	98.72	98.32	94.39	90.01	99.35	98.82	93.03	90.87	99.97	99.95	99.91	99.93
6	Onions	2130	9.58	27.46	86.34	92.79	30.09	63.91	87.98	98.01	22.39	36.05	93.66	94.82	93.66	95.18
7	Wheat	26277	93.59	90.99	98.86	98.49	94.52	90.37	99.53	99.03	93.04	90.64	99.98	99.75	99.92	99.81
8	Beans	1082	65.53	75.91	97.50	99.15	77.08	75.00	98.06	100	63.77	70.99	97.13	98.41	96.40	99.05
9	Peas	2160	78.43	86.43	99.63	99.45	76.94	86.65	99.77	99.68	77.27	87.80	99.95	100	98.19	99.81
10	Maize	1290	64.19	54.37	99.92	94.09	61.71	71.26	99.46	99.07	70.08	57.32	98.29	96.43	98.91	97.70
11	Flax	4301	92.47	94.29	99.09	99.70	91.12	97.39	99.19	99.93	93.56	92.63	99.81	100	99.95	100
12	Rapeseed	28235	92.47	91.53	98.97	98.84	92.73	90.67	99.20	98.79	92.78	91.12	99.96	99.98	100	99.83
13	Grass	4204	68.03	73.73	93.55	95.18	71.86	78.41	96.57	97.01	61.70	80.38	97.03	99.37	99.86	98.96
14	Lucerne	2952	66.53	86.25	94.78	96.65	63.41	88.34	95.22	95.94	68.06	83.05	99.46	98.29	98.81	99.76
Average Accuracy and Average Reliability			**73.08**	**79.18**	**97.43**	**97.78**	**75.37**	**83.78**	**98.00**	**98.79**	**75.34**	**78.74**	**98.87**	**98.99**	**98.91**	**99.16**
Overall Accuracy			**88.37**		**98.46**		**88.99**		**98.98**		**88.38**		**99.65**		**99.68**	
Kappa coefficient			**0.8625**		**0.9819**		**0.8697**		**0.9880**		**0.8628**		**0.9959**		**0.9962**	

Table 5. McNemars test results achieved by 5% training samples.

	SVM (POL)	SVM (POL+MP)	RF (POL)	RF (POL+MP)	1D CNN	2D CNN	3D CNN
SVM (POL)	0	-111.06	-9.11	-116.12	-0.16	-122.47	-122.88
SVM (POL+MP)	111.06	0	107.18	-15.26	111.16	-32.85	-34.79
RF (POL)	9.11	-107.18	0	-112.80	8.73	-118.64	-118.91
RF (POL+MP)	116.12	15.26	112.80	0	116.12	-21.59	-23.68
1D CNN	0.16	-111.16	-8.73	-116.12	0	-122.54	-122.66
2D CNN	122.47	32.85	118.64	21.59	122.54	0	-1.64
3D CNN	122.88	34.79	118.91	23.68	122.66	1.64	0

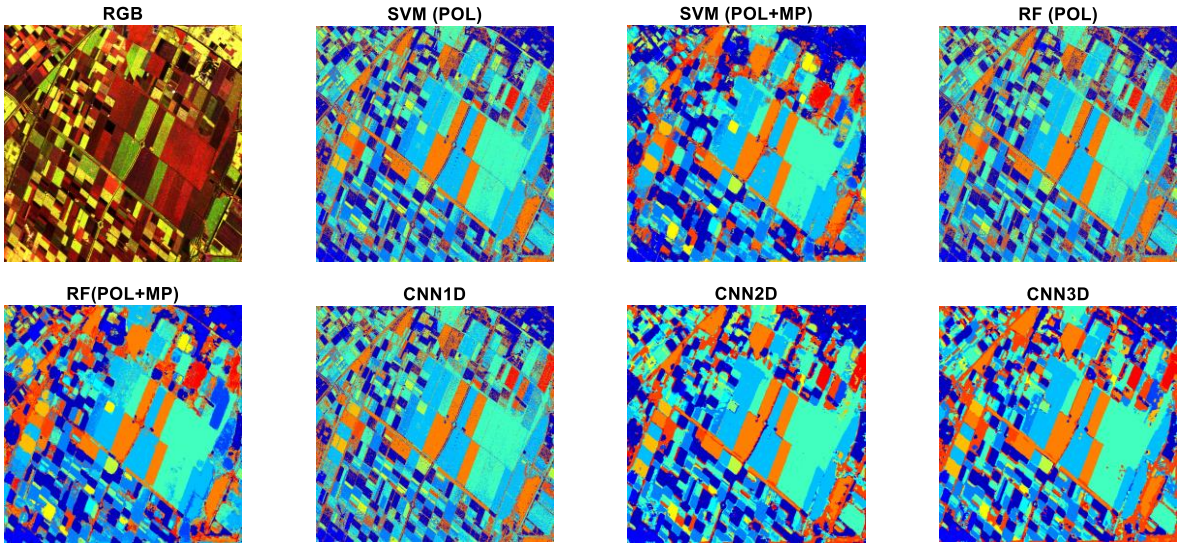

Figure 8. RGB image and classification maps achieved by 5% training samples.

4. Conclusion

Simple CNNs are proposed for dealing with overfitting problem in this work. 1D CNN is not very efficient in PolSAR image classification because it loses the valuable spatial information. Although 2D CNN can be useful in feature extraction and classification of PolSAR image, but, it has not a high capacity in simultaneously polarimetric-spatial features extraction. PolSAR image contains valuable polarimetric-spatial information that can be automatically extracted by 3D CNN. Difference of 2D CNN and 3D CNN is significant from the statistical point of view when limited training samples are used.

References

[1] B. Ren, B. Hou, J. Chanussot and L. Jiao, Modified Tensor Distance-Based Multiview Spectral Embedding for PolSAR Land Cover Classification, IEEE Geoscience and Remote Sensing Letters, vol. 17, no. 12, pp. 2095-2099, Dec. 2020.

[2] O. Harant, L. Bombrun, G. Vasile, L. Ferro-Famil and M. Gay, Maximum Likelihood texture tracking in highly heterogeneous PolSAR clutter, International Geoscience and Remote Sensing Symposium, Honolulu, HI, pp. 4031-4034, 2010.

[3] M. Imani, A Random Patches Based Edge Preserving Network for Land Cover Classification Using Polarimetric Synthetic Aperture Radar Images, International Journal of Remote Sensing, vol. 42, no. 13, pp. 4946–4964, 2021.

[4] R. Hänsch and O. Hellwich, A Comparative Evaluation of Polarimetric Distance Measures within the Random Forest Framework for the Classification of PolSAR Images, IGARSS 2018 - International Geoscience and Remote Sensing Symposium, Valencia, pp. 8440-8443, 2018.

[5] F. Shang and A. Hirose, Quaternion Neural-Network-Based PolSAR Land Classification in Poincare-Sphere-Parameter Space, IEEE Transactions on Geoscience and Remote Sensing, vol. 52, no. 9, pp. 5693-5703, Sept. 2014.

[6] M. Ghassemi, H. Ghassemian, M. Imani, Deep Belief Networks for Feature Fusion in Hyperspectral Image Classification, International Conference on Aerospace Electronics and Remote Sensing Technology (ICARES), Bali-Indonesia, September 20-21, 2018.

[7] Y. Zhou, H. Wang, F. Xu and Y. Jin, Polarimetric SAR Image Classification Using Deep Convolutional Neural Networks, in IEEE Geoscience and Remote Sensing Letters, vol. 13, no. 12, pp. 1935-1939, Dec. 2016.

[8] W. Wu, H. Li, L. Zhang, X. Li and H. Guo, High-Resolution PolSAR Scene Classification With Pretrained Deep Convnets and Manifold Polarimetric Parameters, in IEEE Transactions on Geoscience and Remote Sensing, vol. 56, no. 10, pp. 6159-6168, Oct. 2018.

[9] X. Liu, L. Jiao, X. Tang, Q. Sun and D. Zhang, Polarimetric Convolutional Network for PolSAR Image Classification, in IEEE Transactions on Geoscience and Remote Sensing, vol. 57, no. 5, pp. 3040-3054, May 2019.

[10] M. Imani, Integration of the *k*-nearest neighbours and patch-based features for PolSAR image classification by using a two-branch residual network, Remote Sensing Letters, vol. 12, no. 11, pp. 1112–1122, 2021.

[11] X. Tan, M. Li, P. Zhang, Y. Wu and W. Song, Complex-Valued 3-D Convolutional Neural Network for PolSAR Image Classification, IEEE Geoscience and Remote Sensing Letters, vol. 17, no. 6, pp. 1022-1026, June 2020.

[12] M. Imani, H. Ghassemian, Spectral-Spatial Classification of High Dimensional Images Using Morphological Filters and Regression Model, 6th International Conference on Intelligent & Advanced Systems (ICIAS2016), Kuala Lumpur, Malaysia, 15-17 August 2016.

[13] Z. Zhang, H. Wang, F. Xu and Y. Jin, Complex-Valued Convolutional Neural Network and Its Application in Polarimetric SAR Image Classification, IEEE Transactions on Geoscience and Remote Sensing, vol. 55, no. 12, pp. 7177-7188, Dec. 2017.

[14] W. Tao, H. Yulin, W. Junjie, Y. Jianyu and L. Daifang, SAR ATR based on Generalized Principal Component Analysis Integrating Class Information, 2009 IET International Radar Conference, Guilin, pp. 1-4, 2009.

[15] M. Imani, H. Ghassemian, Binary coding based feature extraction in remote sensing high dimensional data,Information Sciences, vol. 342, pp. 191-208, 2016
[16] G. M. Foody, Thematic map comparison: Evaluating the statistical significance of differences in classification accuracy, *Photogramm. Eng. Remote Sens.*, vol. 70, no. 5, pp. 627–633, 2004.